

# CHAPTER 1: INTRODUCTION

## 1.1 Higher Mobility Semiconductors

### 1.1.1 Introduction

In the past decade great progress have been made in organic field effect transistors and many attractive applications such as radio frequency identification tags, displays and large area sensors have been proposed and demonstrated . In order to fully enjoy the advantages of organic field effect transistors namely mechanical flexibility and low cost features for large area electronics it is important to develop pentacene based field effect transistor. Tremendous progress in performance of these devices have been achieved , Amongst these organic materials pentacene has been found to have the highest mobilities for hole transport (p channel). Organic semiconducting materials have been synthesized and studied for over five decades [1]. In the 1950s, drift mobility measurements and the photoconductivity response of small molecules such as anthracene were examined [1, 2] and although these materials showed semiconducting properties (i. e., conductivities in the range of  $10^{-9} - 10^{-6} \text{Scm}^{-1}$ ) [3], their performance and stability were poor. However, with drastic improvements in synthesis and processing of new classes of molecules such as conjugated polythiophenes in the past two decades [4], the prospects of commercially using organic semiconductors in applications such as organic light-emitting diodes , field-effect transistors and the solar cells is now greater than ever.

### 1.1.2 Organic Semiconductor

One common feature of organic field effect transistor is inclusion of conjugated pie electron system, facilitating the delocalisation of orbital wave functions electron withdrawing groups and donating groups can be attached that facilitate hole or electron transport. Semiconductors based on organic molecular components are mainly composed of hydrogen, carbon, and oxygen. Unlike inorganic semiconductors that are crystalline with band-like charge transport, organic semiconductors are amorphous or polycrystalline in which the charge transport occurs through hopping of charges between delocalized  $\pi$  molecular orbitals.

As the essential material for organic electronics, organic semiconductors have attracted huge attention for over three decades, and emerged as the commercial alternative to conventional inorganic semiconductors such as silicon. Unlike inorganic materials the organic

semiconductors have the physical and chemical properties that can be easily tailored by the incorporation of the fundamental groups or the manipulation of physical conditions to meet the specific requirements. The versatility of these materials afford a brand new era for the development of novel electronic devices and poises to revolutionize the society. Numerous pie conjugated organic semiconductors have been synthesised and successfully used in organic electronic devices.

One advantage of the organic semiconductors over the inorganic ones is the low requirements of the processing conditions. Most inorganic semiconductor devices are prepared on the high purity crystalline substrates at high temperature, normally relying on the utilization of expensive facilities in clean rooms.

The semiconducting or conducting properties of organic molecules can be attributed to the special chemical characteristic of carbon: carbon atoms can form double bonds between each other, as shown in Figure 1.1. One is known as a  $\sigma$  bond formed by the overlap of hybridized  $sp^2$  orbitals, and the second is known as a  $\pi$  bond formed by the overlap of the remaining unhybridized  $p_z$  orbitals. The  $\sigma$  electrons always remain between the carbon atoms, while the  $\pi$  electrons are delocalized over the neighboring molecules in a conjugated system, by which the electrons can gain some freedom to move along the entire chain. The formation of delocalized  $\pi$  molecular orbitals defines the frontier electronic levels: the highest occupied molecular orbital and the lowest unoccupied molecular orbital. The HOMO and LUMO levels determine the electrical and optical properties of the organic semiconductor molecules.

Based on different basic units, organic semiconductors can be categorized into two groups: small-molecule organic semiconductors and polymer organic semiconductors. In small molecule organic semiconductors, the carbon atoms form larger molecules typically with benzene rings as the basic unit and  $\pi$  electrons become delocalized through the molecules, as shown in Figure 1.2(a). The molecular weight of small-molecule semiconductors is usually less than 1000 g/mol. In polymer organic semiconductors as in Figure 1.2(b), the carbon atoms form a long chain and  $\pi$  electrons become delocalized along the chain and form a one dimensional  $\pi$ -conjugated system. The molecular weight of polymeric semiconductors is usually greater than 1000 g/mol.

### 1.1.3 OFET

Ofets have the source, drain and gate electrodes similar to their inorganic counterparts. Being absent of a depletion region, an OFET normally operates in an accumulation region and the low off current in the device is dominated by the inherent conductivity of the active layer. When a gate voltage is applied, the channel current flowing through the organic semiconductor film can be modulated by field-effect doping process.

In which  $I_{DS}$  is the channel current between source and drain  $W$  and  $L$  are the width and length of the channel respectively,  $\mu$  is the mobility of the carrier,  $C_i$  is the capacitance of the gate insulator,  $V_g$  is the gate voltage,  $V_{DS}$  is the applied source drain voltage and  $V_t$  is the threshold voltage of the device. Therefore the channel current of the ofet based sensors could be primarily modulated by the two parameters in the above equations namely threshold voltage and carrier mobility, which both play significant role in sensing applications. The threshold voltage of the device is normally changed by the doping effect upon to the exposure to the target analytes while the carrier mobility is influenced by the analyte molecules diffused into the semiconductor grain boundaries.

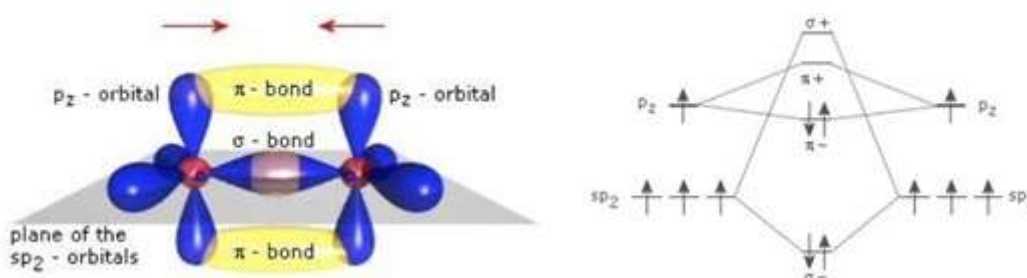
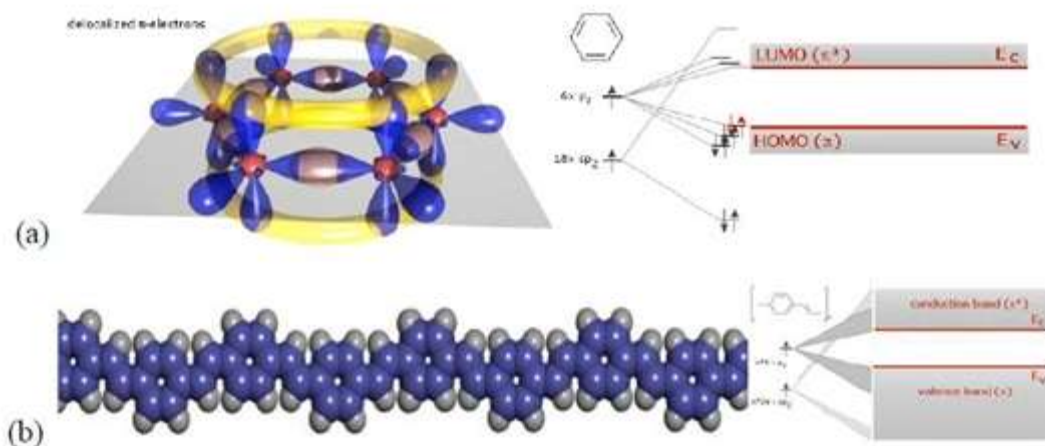


Figure 1-0-1: Scheme of the orbitals and bonds for two  $sp_2$  hybridized carbon atoms [5]



**Figure 1-0-2 (a) Scheme of a benzene ring and energy structure of small-molecule organics. (b) Scheme of a polymer subunit and the energy structure of polymer organics [5].**

The discovery of electrical conduction in organic solids dates back nearly 100 years with the observation of photoconductivity and the study of the dark conductivity in anthracene crystals [6,7]. In 1977, the first highly conducting polymer, chemically and electrochemically doped polyacetylene, was discovered by Heeger, Shirakawa, and MacDiarmid, which won them a Nobel Prize in Chemistry in 2000 [8]. This remarkable observation opened up an entire new field called organic electronics, and a new range of applications for conducting and semiconducting organic materials. Organic electronics generally refers to electronic devices and systems that are based on organic semiconductors, and generally it is applied to three main technological areas: organic light-emitting devices (OLEDs), organic photovoltaic solar cells (referred as OSCs or OPVs), and organic electronic circuits based on organic thin-film field effect transistors (referred as OTFTs or OFETs). In May 2008, Sony unveiled an ultra-thin 11 inch OLED TV with high energy efficiency and brightness [9]. OLEDs could compete with and eventually replace white and blue GaN-based light-emitting diodes (LEDs) used in mobile phone displays since they do not require backlighting. OPVs are envisioned as future power supplies for large-scale power generation [10]. OFETs have recently gained attention as building blocks for electronic applications that can greatly benefit from lowcost, large-area fabrication and flexible form factors, such as radio-frequency identification tags (RFID) [11], drivers for electronic paper [12] and driving circuits for flat panel displays (FPDs) [13].

#### **1.1.4 OFET vs Inorganic FET**

OFETs, thin-film transistors (TFTs) with organic semiconductors as the active layers, are of

great interest as a potential alternative to amorphous Si ( $\alpha$ -Si) TFTs. With remarkable progress in the synthesis and purification of organic semiconductors and the processing of these materials into devices, the mobility of the best OFETs has surpassed that of  $\alpha$ -Si TFTs [14].

A major advantage of OFETs vs.  $\alpha$ -Si TFTs is their compatibility with low-cost, low temperature processes. A typical  $\alpha$ -Si:H TFT fabrication process involves the deposition of hydrogenated  $\alpha$ -Si as an active layer and silicon nitride as a gate dielectric by plasma enhanced chemical vapour deposition (PECVD) using  $\text{H}_2/\text{SiH}_4$  (silane) and  $\text{NH}_3/\text{SiH}_4$ , respectively. The process temperature is usually much higher than 250 °C, which enables the use of inexpensive glass as substrate [15]. However, this fabrication process is not compatible with colorless, transparent flexible polymeric substrate materials, which typically require a temperature below 200 °C. OFETs, on other hand, can be processed at much lower temperatures using various simple, low cost techniques, including vacuum thermal evaporation, spin-coating, dip-coating, vapor deposition, microcontact printing, screen printing, etc. The combination of low-temperature processibility with the mechanical flexibility of organic materials thus leads to a wide range of applications in flexible electronics with a potential for very low cost manufacturing.

Secondly,  $\alpha$ -Si technology provides only high performance  $n$ -channel transport which prevents the use of complementary metal-oxide-semiconductor (CMOS) technologies. In contrast, the versatility of synthetic organic chemistry has enabled the tailoring and engineering of both  $n$ - and  $p$ -type semiconductors, giving rise to many potential candidates for circuit designs based on CMOS technology.

## **1.2 Organic Field-Effect Transistors**

### **1.2.1 Introduction**

Organic Field Effect Transistor (OFETs) is transistor which using organic semiconductor in channel. OFETs have been of great interest for applications, such as display drivers, identification tags and smart cards, because they have advantages of low cost, flexibility and light weight printed electronics, electronic paper (e-paper), electronic skin, etc [16]. A good example of this progress is a 5-order of magnitude increase in the field-effect mobility from 1986 to present [16], making the organic electronic devices a viable replacement for amorphous Si devices.

Despite of improvements in fabrication and characterization of thin-film organic field-effect transistors, the physics of charge injection and transport in these devices is not well understood. Before we discuss these issues in detail, a basic review of the transistor's mode of operation and the different charge injection mechanisms is essential.

### 1.2.2 Operating mode

OFETs are having four modes these are top contact bottom gate(TCBG), bottom contact bottom gate(BCBG), top contact top gate(TCTG) and bottom contact top gate(BCTG). Out of these two are very common TCBG and BCBG.

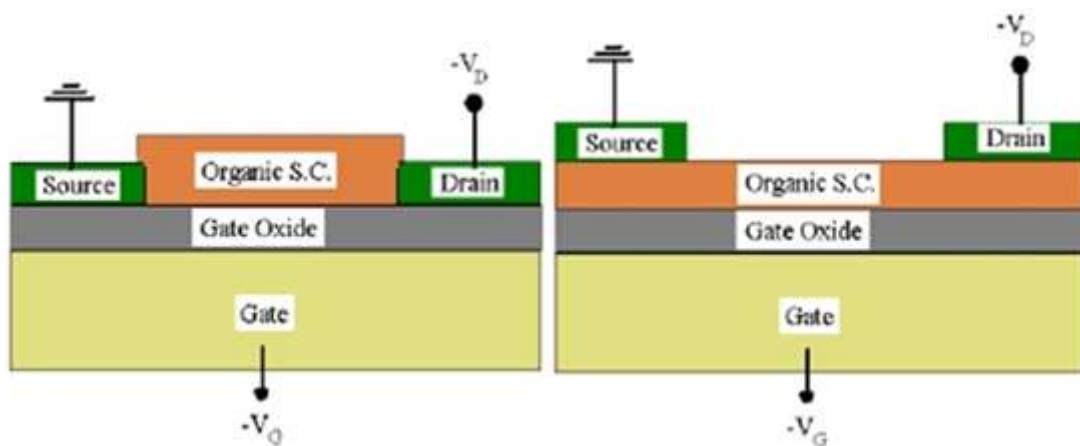


**Figure 1-0-3(left): A schematic view of a bottom contact OFET. The source electrode is grounded, while the drain and the gate are biased negatively. In this mode, holes are injected from the source and collected at the drain. (right): A top contact OFET with the electrodes patterned on top of the organic polymer**

OFET works in accumulation mode. When gate voltage is applied a charge layer is formed in between this oxide layer and organic layer. This help in current flow when drain voltage is applied. There is a advantage of top contact geometry contact area is large between electrode and organic semiconductor, as compared to the BCBG. But there is one disadvantage also making contact over the semiconductor can damage it, so a safe approach is necessary. Therefore, top contact design is not frequently used.

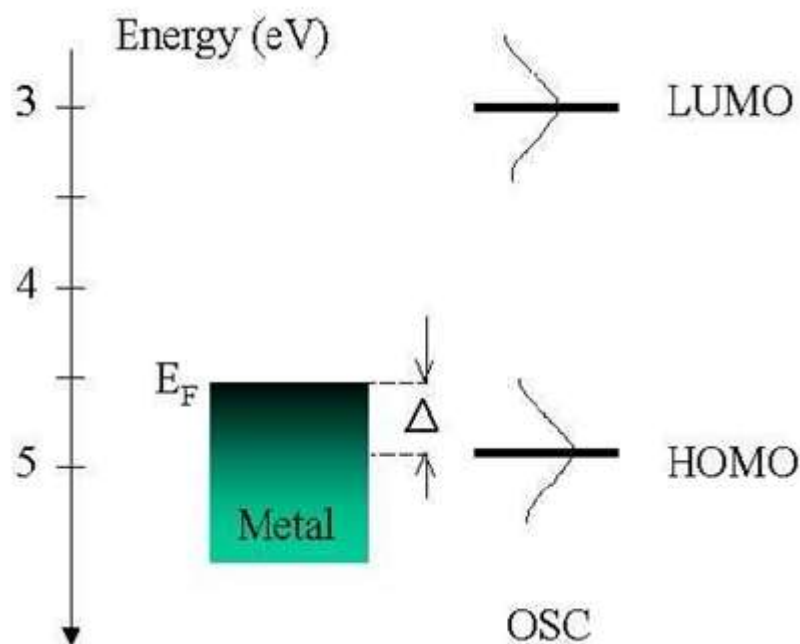


Figure 1-0-4 The energy diagram showing the band alignment at an OSC/metal interface such as Au/pentacene. Holes are injected from the Fermi level of the metal into a Gaussian energy-dependent state in the HOMO, overcoming an intrinsic energy barrier  $\epsilon$  (adapted from Ref. [3]).

Most OFETs reported in the literature so far show either p-type or n-type behaviour, meaning that the charge carriers are either holes or electrons respectively. P-type OFETs comprise the majority of these devices, showing the best transport properties. However, Very recently, a few groups [17, 18] have shown that ambipolar charge transport is also quite achievable and is a generic property of the OSCs. This can pave the way for fabrication of organic complimentary metal-oxide semiconductor (CMOS) logic circuits.

## 1.3 Mechanisms of Charge Injection and Transport in Organic Semiconductors

### 1.3.1 Introduction

The performance of the organic electronic devices, including thin film field-effect transistors and organic light emitting diodes (OLEDs), depends on the nature of charge injection from the contacting electrodes into the OSC, followed by the effective transport of the carriers through the bulk of the material. In light emitting diodes [19], the effective injection of the holes and electrons from the contacts is followed by transport. Through the bulk, leading to recombination and emission of light. In solar cells [19], holes and electrons are generated upon absorption of light, followed by transport through the device and collection at the electrodes, and in FETs, charge injection at the source is followed by transport through the

channel and collection at the drain. Since the underlying principle of operation in all these devices is similar, we will review the different mechanisms of charge injection and transport in the following sections.

### **1.3.2 Bulk-limited transport**

If the contact between the metal and the OSC is Ohmic, with a contact resistance much lower than the resistance of the bulk material, then the current will be easily injected into the organic material and the transport of charge will be dominated by the bulk [19]. By Ohmic contact we mean the electrode, being an infinite reservoir of charge, can maintain a steady state space-charge limited current (SCL) in the device [4]. In the case where the injected charge dramatically changes the electric field configuration in the polymer (i.e., effectively screens the source-drain field) the transport becomes space-charge limited. In this case, the  $I$ - $V$  curves look linear if the field due to the applied bias is the dominant  $E$  field in the device. The conduction is usually linear in the low source-drain bias since the current density in the polymer is low. At higher fields where the current density is very high, there is a significant concentration of charge carriers in transit between the source and the drain. The screening due to these “space charges” produces nonlinear  $I - V$  characteristics.

It is important to note that space-charge effects are more readily maintained in materials such as organic semiconductors where the mobility is poor. The low mobility greatly restrains the collection of the carriers at the drain or the recombination of opposite charges. In addition to these effects, OSCs are known to have large concentration of highly localized states (i.e., traps, defects etc) that trap mobile charges temporarily or permanently (immobile charges) [4]. All these factors make organic semiconductors the perfect breeding ground for space charge transport.

### **1.3.3 Hopping nature of transport in organic semiconductors**

The presence of defects and the non-crystalline structure of the organic polymers leads to the formation of localized states. In order to move, charges must hop between these localized states and overcome the energy difference between them, emitting or adsorbing phonons during intra-chain or inter-chain transitions [13].

In OSCs, the constituting molecules are only weakly bound together through van der Waals forces and the traditional view of band formation is not very accurate. In these materials,



band energy widths are typically smaller than  $k_B T$  [4].

In this simple picture, a carrier is initially localized at a particular energy site  $i$ , confined approximately within a deep or shallow potential well. Upon receiving enough thermal energy, the carrier can overcome the potential barrier and hop over to a neighbouring site,  $j$ . This process is illustrated by Fig. 1.5. Thermally assisted hopping is the dominant mechanism of transport in organic semiconducting materials. Therefore, the mobility and hence the conductivity of (disordered) OSCs exponentially increase with temperature, which is different from temperature dependence of conductivity in crystalline semiconductors such as Si or Ge. The picture of hopping described above is greatly simplified. In reality density of states and the possibility of both short and long range hops to neighbouring sites should be considered [18].

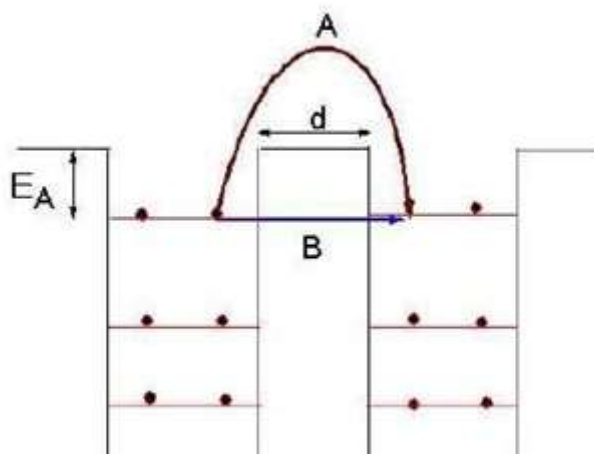


**Figure 1-0-5 Two mechanisms of charge transfer between two localized states: A) Hopping of a charge carrier from one localized state to another upon receiving enough energy to overcome the activation energy barrier  $E_A$ , and B) direct tunnelling between the 2 states.**

### 1.3.4 Injection-limited transport

In addition to the intrinsic (bulk) properties of the semiconducting polymers in transporting the electronic charge, the interface between the OSC and the contacting electrode (usually a electronic devices. If the bottleneck in charge transport is injection at the contacts, a device is said to be injection or contact limited. In this case, the metal/OSC interface may show Ohmic or nonlinear I–V characteristics. The band offset between the metal work function and the HOMO or LUMO level in the OSC (depending on whether the transport is p- or n-type) is one important factor in determining the type of contact at the interface [3,20]. If there is a sizable potential energy barrier from the metal into the transporting band in the OSC, the charge

injection would be poor and the contact resistance will dominate the device operation. However, many factors such as electrode work function, doping levels, interfacial traps or dipoles etc. influence the band alignment at the interface.

Chapter 2 Literature review, contain review of gate dielectric material, influence of higher gate dielectric which reduce the threshold voltage. Flexible gate dielectric for flexible application like display and many more. Threshold voltage and its dependency. Some other application of OFET. conclusion

Chapter 3 Pentacene, structure of pentacene. Charge transport in pentacene, one of that is space charge limited current. The influence of non-idealities on charge transport like trap, electrode material and electrode geometry. Why pentacene is P-type.

Chapter 4 Methodology contain which method is used to find  $I_d$ - $V_g$  characteristics of OFET. ATLAS is used in the simulation of OFET.

Chapter 5 Result and Discussion contain the channel length modulation. What happen when channel length is varied. Effects on the  $I_d$  - $V_G$  graphs

Chapter 6 Conclusion and future prospects.

## CHAPTER 2: LITERATURE REVIEW

The principle of the field-effect transistor (FET) was first proposed by Lilienfeld in 1930. First descriptions of the field effect in organic semiconductors was on 1970, organic FETs (OFETs) have only been identified as potential elements of electronic devices the report by Koezuka and coworkers, in 1987, on a structure based on electrochemically polymerized polythiophene. Polythiophene belongs to the family of conducting (or conjugated) polymers (CPs) that were discovered in the late 1970s.

Now a days small conjugate molecule are also promising material for this application. The performance of OFETs has continuously improved since then, and some OFETs now compete with amorphous silicon FETs, which are now preferred to conventional crystalline silicon FETs in applications where large areas are needed[21].

### 2.1 Gate Insulator

Different dielectric plays different role in OFET. As in inorganic transistor gate insulator used are  $\text{SiO}_2$ ,  $\text{Al}_2\text{O}_3$ , and  $\text{HfO}_2$ , various organic materials were also tried for the gate dielectric in OTFTs. In addition, polymethyl methacrylate (PMMA) derivative polymers are one of the new materials for the gate dielectric or buffer layer, exhibiting high field effect mobility and low threshold voltages. Miskiewicz *et al.* have demonstrated that the surface energy of the dielectric can have large impact on the performance of FETs based on TTF-4SC18 [22]. Average charge carrier mobility was 30 times increased as a result of proper treating.

### 2.2 Influence of higher dielectric constant

To use high dielectric constant proper interaction for organic layer and strength is necessary. Another advantage of high materials is a lower operating voltage. There has been shown very clearly the beneficial role that plays the high dielectric constant tantalum oxide ( $\text{Ta}_2\text{O}_5$ ) as a gate insulator in OFETs. It has been shown that using high gate structure provides possibility of injection a higher amount of charge carriers into organic active layers than on the  $\text{SiO}_2/\text{Si}$  gate conventionally used in most OFETs.

### 2.3 Gate dielectrics on flexible substrates

Generally we use  $\text{SiO}_2$  for OFET, and this is grown over inflexible substrate. To make it

flexible for flexible electronics, Parashkov *et al.* have fabricated fully patterned all organic TFTs with a variety of organic polymer insulators and the gates printed on top of the gate dielectric layer. The group has produced OTFTs on flexible polyimide substrates and obtained devices with electrical performance similar to that of OTFTs fabricated with inorganic gate dielectrics and metal contacts.

Majewski *et al.* have investigated bottom-gate OFETs using a commercially metallized Mylar films coated with an ultra-thin (3.5 nm) SiO<sub>2</sub> layer as a flexible substrate. The OFETs have been fabricated using this substrate, region regular poly(3-hexylthiophene) (rr-P3HT) as a *p*-type semiconductor, and gold source and drain contacts. This resulted in OFETs that operated with voltages of the order of 1 V.

## 2.4 Threshold voltage

The threshold voltage  $V_T$  is an important parameter that needs to be controlled to ensure proper operation of the circuits.  $V_T$  can depend on the time a gate voltage has been applied (bias stress), on the exposure of the device to light, it can be shifted using a polarizable gate insulator or it depends on thickness of the semiconductor layer. Furthermore, a dependence on the work function of the gate electrode has been reported.  $V_T$  voltage additionally has been found to depend strongly on the preparation of the surface on which the organic material is deposited. Threshold voltage shifts in thin film as well as single-crystal OFETs have been found to be induced by dipole monolayers on the gate insulator[22]. Thickness of the semiconductor layer influences the values of the threshold voltage and, to a lesser extent, the saturation current. The thickness-dependent part of the threshold voltage results from the presence of an injection barrier at the gold-pentacene contact.

## 2.5 Field Effect Mobility

Mobility is generally used to measure the device performance. Mobility of the OS thin film is receiving significant attention for transistor characteristics and a reliable operation of the transistor requires larger mobility. Compared with inorganic semiconductor material devices, polymeric and small molecules based OFETs have mobility ranging from 10<sup>-6</sup> to 1 cm<sup>2</sup>/V.s. Pentacene is the most widely used OS for organic transistors due to its higher hole mobility. The Pentacene-based OTFTs have a field effect mobility of around 1 cm<sup>2</sup>/V.s. This is of comparable value to hydrogenated amorphous silicon.

## 2.6 Applications of OFETs

In the research point of view OFET is still under improvement. There are lot of applications some of them are presented here memory and logic elements, LCD panel driven OTFT and OFETs as chemical sensors. Anthopoulos *et al.* [25] have shown that organic transistors based on the solution processible methanofullerene [6,6]-phenyl-C<sub>71</sub>-butyric acid methyl ester exhibit promising ambipolar charge transport characteristics. This structure was found to allow the realization of logic circuits with good noise immunity. Pinto *et al.* [26] have shown that a spin coated rr-P3HT single channel split gate OFET functioned as a dual input logic “AND” gate with an order of magnitude higher mobility. A significant advantage of this architecture is that „AND“ logic devices with multiple inputs can be fabricated using a single rr-P3HT channel with multiple gates. The reversible memory effect due to extrinsic trap states and the bias stress effect originate from totally different mechanisms and can be separated in data analysis [27].

Write-once-read-many-times (WORM) memory devices have been demonstrated using a material system of polyethylene dioxythiophene:polystyrene sulphonic acid and a con-jugated copolymer containing fluorene and a chelated euro- pium complex. Some rewritable devices are characterized by embedding nanoparticles, while others are characterized by the intrinsic memory effects of the materials. The former devices are nanoparticle-based organic memory units in which the organic materials themselves have no memory effects. This flexibility provides, in a single class of material, the ability to achieve complementary logic and even devices such as *p-n* diodes and more complex systems. Complementary inverter based on interface doped pentacene has been shown to be promising device, which has been demonstrated in[28].

Hur *at al.* [21] have studied *p*-channel, *n*-channel, and ambipolar SWNT FETs with electrodes defined by a high-resolution printing process. Complementary logic gates with these types of devices illustrate their suitability for complex circuits.

Functionalised Graphene electrodes are also used for transparency, light weight and flexibility. The next generation will be of organic because its fabrication is much easier than Si. printable circuit and ink jet printable circuit is possible. You are able to print the circuit anywhere on a plastic substrate.

## 2.7 Conclusions

Many groups demonstrated the important functionalities of organic gate dielectrics and their effect on the output performance of OFETs. For instance the polymer dielectric that was directly attached to the pentacene layer governed the transport and accumulation of charge carriers. The mechanisms by which PVA facilitates the formation of the  $n$  channel in the pentacene active layer biased in the accumulation at the positive  $V_G$  regime are not completely established as yet. There has been shown very clearly the beneficial role which plays high dielectric constant  $\text{Ta}_2\text{O}_5$  as a gate insulator in OFETs.

In order to conduct research on physical effects occurring in organic semiconductors, most recent works involving OTFTs have typically employed the selective deposition of metallic conductors through a shadow mask or vacuum deposition followed by photolithographic patterning, an approach that is both time consuming and costly. Hence, it is highly desirable to achieve high-performance especially  $n$ -channel OFETs that can be processed at room temperature using standard physical vapour deposition. Light emission from an OFET requires ambipolar transport, as well as efficient radiative decay. Recent experiments have demonstrated ambipolar channel conduction and light emission in conjugated polymer FETs. These achievements make realistic fabrication of suitable in commercial applications the complex active matrix with organic light-emitting diodes (AMOLEDs) [29].

## CHAPTER 3: PENTACENE

Pentacene (from penta=5 and acene=poly cyclic aromatic hydrocarbons with fused benzene ring) is a flat like molecule made up of five linearly fused benzene ring. Interest in pentacene has grown dramatically in recent years as a result of both crystal and thin film behaving as a p-type organic semiconductor which can be employed to manufacture electronic device such as the organic field effect transistor (OFET).

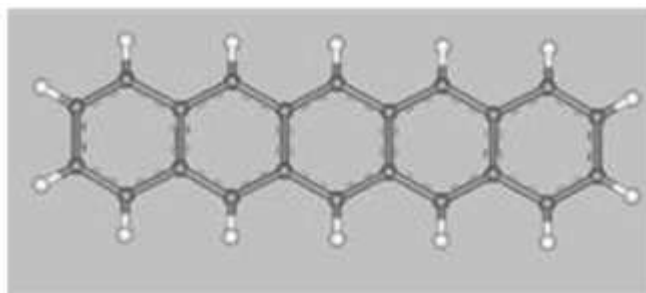


Figure 3-0-1Pentacene

### 3.1 Structure

Pentacene ( $C_{22}H_{14}$ ) contains only carbon and hydrogen atoms. Its structure is represented in figure 3.1. Pentacene belongs to a group of molecules called polycyclic aromatic hydrocarbons[30]. Molecules of this group have several hydrocarbon rings in which the carbon atoms are alternatingly connected by carbon double and single bonds. More specifically, pentacene is the fifth member in the group of fused benzene rings in a linear arrangement, called the acenes. The first four members are benzene, naphthalene, anthracene and tetracene. Above five rings a linear arrangement becomes less stable and therefore less abundant. The alternation of double and single bonds, also called conjugation, is a result of a specific atomic electronic configuration. In general the electronic configuration of carbon is given by  $2s^2 2p^2$ . In conjugated structures two of the three p orbitals of the carbon atom hybridize with the s orbital to form 3 spatially localized orbitals. The three orbitals are located in the same plane and the angle between the orbitals is equal,  $120^\circ$ . These orbitals are mainly responsible for chemical bonding between carbon atoms. The p orbital left, usually called the p<sub>z</sub> orbital, is spatially localized above and below this plane. In conjugated systems these p<sub>z</sub> orbitals also contribute to chemical bonds in the plane. However, such a bond is much weaker than bonds made from the hybridized orbitals. Therefore, these electrons can also contribute in electronic conduction. This explains the relatively high conductivity of a sheet of graphene. Thermodynamically speaking, pentacene is quite stable.



When storing at room temperature in air only one significant impurity species will form, 6,13-pentacenequinone. This species is quite different from pentacene itself due to the attachment of two oxygen atoms and has lost its full conjugation. The quinone can be removed by vacuum sublimation. Pentacene is a crystalline solid at room temperature. In general, pentacene crystals have a triclinic crystal system and have four distinguishable Phases or symmetries [31]. Crystals are composed of layers, in which the long axis of the molecule is oriented almost perpendicular to the plane of the layer. In-plane pentacene molecules are arranged in a herringbone-like way. The relative orientation of the hydrogen atoms between molecules and the angle of the long axis with respect to the plane determine the specific phase of the crystal. Phases are characterized by the spacing between stacked layers,  $d$ . The four phases are characterized by  $d$ -values of 1.41 nm, 1.45 nm, 1.50 nm and 1.54 nm. Thin films structures can depend on temperature and substrate and the 1.41 nm is most likely to form. Single crystals of pentacene can be grown by vapour transport growth [32]. Thin films of pentacene show an island-type growth mode (Stranski Krastanov), resulting in thin films composed of crystalline grains with typical dimensions of several micrometers depending on substrate and substrate temperature during or after deposition [33].

## **3.2 Charge transport**

### **3.2.1. Space charge limited current**

How to think about charge transport in pentacene? Lets consider the problem in a band picture. Pentacene has a filled valence band (or in molecular terms highest occupied molecular orbital, HOMO) separated from an empty conduction band (in molecular terms lowest unoccupied molecular orbital, LUMO) by a band gap of 2.2 eV which is much larger than  $k_B T = 0.03 \text{ eV}$  (298K). One can inject carriers by either injecting electrons in the conduction band or holes in the valence band. We consider one carrier injection, since pentacene is a hole conductor, or p-type semiconductor.

Metals, usually have a lot of intrinsic carriers which are free to move throughout the material, since there are many empty states just above the Fermi level. Pure semiconductors have a band gap and the the number of charge carries is limited. Injecting a charge carrier in a semiconductor will give rise to a so called space charge. An increase in the electric field will inject more charge carriers, which space charge will increase the electric field even more giving rise to a current which is quadratically dependent on voltage. The current will be bulk

limited. This is in contrast to Ohmic conductors which have a linear dependence on voltage and are injection limited. The quadratic behavior is also known as space charge limited current (SCLC)

### **The influence of non-idealities on charge transport**

This section will qualitatively describe the influence of three non-idealities on charge transport in pentacene:

- The influence of traps
- The influence of the electrode geometry
- The influence of the electrode material

#### **Traps**

The band model above assumes a SC with a gap without (impurity) states in the gap. In reality states will be present. For pentacene thin films the most well known impurities causing trap states in the band gap are water, oxygen and grain boundaries between crystalline islands [32] [34] [35] [36] [37]. The effects of water and oxygen on charge transport are described by Jurchescu et al. [34]. Air can reversibly diffuse in pentacene and affects electrical transport significantly. Water reduces electrical transport, because its electric dipole induces energetic disorder and traps charge carriers. Oxygen on the other hand enhances electrical transport and attracts electrons, thereby forming holes. The effect of oxygen can even be enhanced in the presence of light. When exposing a pentacene layer in ambient air to light, current increases by about a factor of two. The polycrystallinity in pentacene thin films causes a non uniform dielectric medium. Minari et al. [38] report an enhancement of mobility (and current) in pentacene thin-film transistors when they are made from a single grain as compared to polycrystalline ones.

#### **Electrode geometry**

To investigate charge transport one can contact a material in several ways. Because of the relative high resistivity of organic SCs, the contact resistance and the resistance of the leads can often be neglected. The most straightforward way of applying contacts to a piece of material is to clamp a thin sheet of material between two electrodes such that the current is flowing perpendicular to the sheet. A major advantage of this geometry is the electric field uniformity. Also, one can easily make large contact areas ( $A$ ) and thin films ( $L$ ) such to increase the total current, since  $R \propto L/A$ . Another geometry can be obtained by connecting a sheet of material laterally. In a lateral geometry, the electrodes are attached on top or below

the sheet of material such that the current is flowing in the plane of material. The ultimate advantage of this geometry is that one can use multiple electrodes, which is one of our demands. However, the conductance path in this geometry is not well defined since the electric field is not completely homogeneous [39]. The non-uniformity of the electric field in a lateral geometry is caused both by the electrode shape, usually a strip with sharp edges, and by the influence of the substrate. Lateral geometries can be made either by applying electrodes on top or below a film. Applying electrodes on top of pentacene might damage the pentacene [40].

### Electrode material

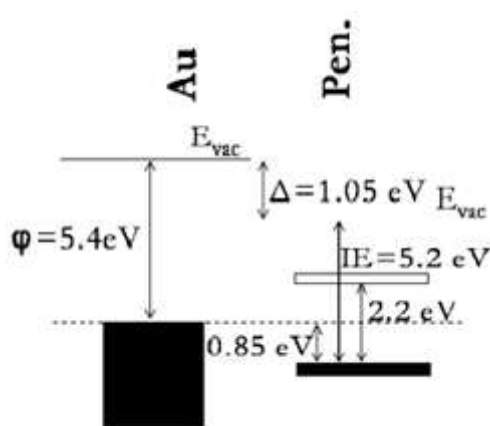


**Figure 3-0-2** Band pictures of pentacene connected to gold. The band picture predicts the effective hole injection barriers. The Fermi level is indicated by the dotted line. Gold data is obtained from Koch et al. IE is the ionization energy and  $\phi$  is a dipole that arises at pentacene-metal interfaces, which will effectively change the vacuum level.

Pentacene is a hole conductor, since the cation of pentacene (a pentacene molecule missing one electron) is more stable than the anion of pentacene (a pentacene molecule with one additional electron). The easiest way to inject holes in pentacene is to connect it with an electrode of which Fermi level is close to the HOMO of the pentacene. We use the same electrode material for the cathode and the anode gold. Schematic energy diagrams of these three situations without bias are given in figure 3.2. In this picture we assume that pentacene maintains its molecular properties, such that the levels are not broadened. Due to a dipole at metal-pentacene interfaces the electrons in both materials experience a different vacuum level. This dipole is formed due to electron transfer from pentacene to the metal. The contacts in the simplified model of figure 3.2 are clearly non-Ohmic and a hole injection barrier appears of  $0.85 \text{ eV}$  for a gold/pentacene interface. When introducing a tunnel barrier in between the metal and the pentacene, a dipole will be formed between the oxide and the pentacene. However, the dipole between the pentacene is strongly reduced [41]. Now, charge carriers can cross this barrier by an inelastic tunnel process. In the band

picture, at high positive biases a triangular shaped electron barrier arises and one might expect electron injection. Pentacene field effect transistors using both hole and electron injection contacts report pronounced increase of drain currents at large values for the drain source voltage [42] [43].

Pentacene is having both  $e^-$  and holes, both can move freely in the pentacene. Hopping of these is by quantum mechanical tunnelling effect. Electron mobility is much lower and even negligible in air for two reasons.

1. Electron in its lowest unoccupied molecular orbital LUMO is very reactive to  $H_2O$  molecule which is present in ambient air.
2. Hydroxyl group R-OH at semiconductor insulator interface to act like  $e^-$  trap which immobilize the negative charge carrier.

Therefore pentacene is p-type only.

Pentacene is most commonly use material in OFET because mobilities for pentacene OFET ranges between  $0.1\text{cm}^2/\text{Vs}$  and  $1\text{cm}^2/\text{Vs}$  have been reported by many groups worldwide. In spite of enormous activities in synthesising and screening for new material for transistor application, pentacene has successfully defended its leading position for the production of OFET[44].

## CHAPTER 4: METHODOLOGY

### 4.1 Introduction

Simulation of OFET is done with the help of ATLAS. ATLAS provides facility for physically-based two (2D) and three-dimensional (3D) simulation of semiconductor devices. It predicts the electrical behaviour of specified semiconductor structures and provides insight into the internal physical mechanisms associated with device operation.

### 4.2 ATLAS Inputs and Outputs

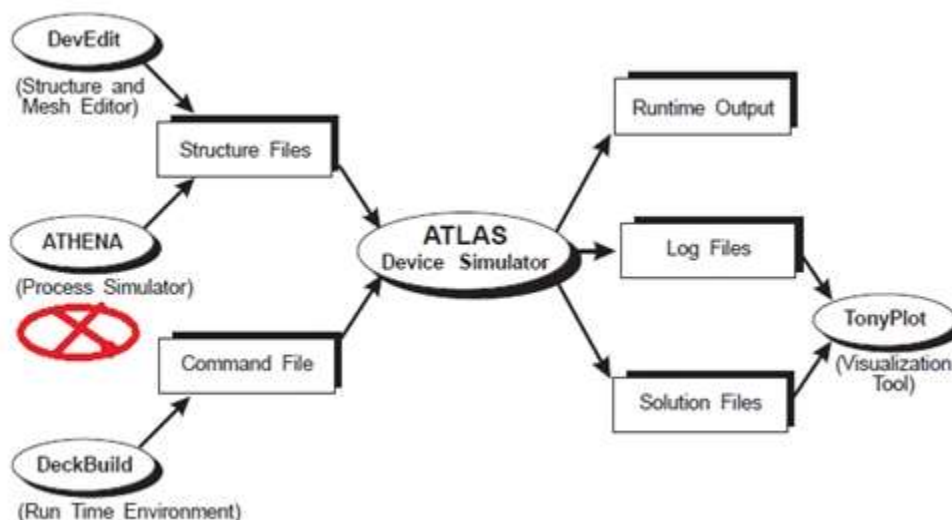


Figure 4-0-1 ATLAS input and output

Most ATLAS simulations use two input files. The first input file is a text file that contains commands for ATLAS to execute. The second input file is a structure file that defines the structure that will be simulated. ATLAS produces three types of output files. The first type of output file is the run-time output, which gives you the progress and the error and warning messages as the simulation proceeds. The second type of output file is the log file, which stores all terminal voltages and currents from the device analysis. The third type of output file is the solution file, which stores 2D and 3D data relating to the values of solution variables within the device at a given bias point[45].

Structure is build in DevEdit and command files are written in Deckbuild. Models used in this simulation are drift diffusion model and hopmob pfmob they are models for organic semiconductor.

## CHAPTER 5: RESULT AND DISCUSSION

Higher contact length ( $L_C$ ) reduces contact resistance but large contacts (sometimes as large as a millimeter) greatly increase the device size and consume more contact material (e.g., Au). Here, we take top contact OFET and bottom contact OFET for contact length variation. Parameters use in the structure of the OFET are length of the device is 90 micro meter. Width of the gate is 20 nano meter and material of gate electrode is aluminium, width of the gate oxide is 280 nano meter material used in the gate oxide is  $\text{SiO}_2$ , organic material is pentacene thickness of pentacene is 100 nano meter, source and drain thickness is 20 nano meter or less length is varied over 10 micro meter to 40 micro meter. Both the case top contact and bottom contact the parameters are same.

$L_C$  is the length of the source and  $L_{C0}$  is the characteristic length  $R_s$  is the source resistance  $R_{ch}$  is channel resistance. The influences of the contact length ( $L_C$ ) on the contact resistance ( $R_{sd} = R_s + R_d$ ) and the channel resistance ( $R_{ch}$ ). First, large  $L_C$  indeed decreases  $R_{sd}$ , but  $R_{ch}$  as well. The latter result indicates the alleviated contact limitation to channel transport achieved by providing larger injection area. Second, the strong dependence of  $R_{sd}$  on  $L_C$  is more observable at high  $V_G$ . This is in line with the largely reported current crowding, by which the effective charge injection area balances  $R_{sd}$  and  $R_{ch}$ . As  $V_G$  is increased,  $R_{ch}$  decreases faster than  $R_{sd}$  and the injection area is enlarged to maintain the balance, resulting in a smaller  $R_{sd}$ . At a small  $V_G$ ,  $R_{sd}$  decreases slightly upon expanding  $L_C$  whereas more than 60% decrease in  $R_{sd}$  can be obtained at high  $V_G$ . Over the critical length  $L_{C0}=0.6\mu\text{m}$ , further expanding increases the parasitic capacitance that will adversely affect the performance[48].

We found that  $L_{C0}$  strongly depends on the OSC film thickness  $t_{SC}$  with larger  $L_{C0}$  for thicker films. Interestingly,  $L_{C0}$  for four different film thicknesses nearly follows the same relationship as  $L_{C0} = 6t_{SC}$  since  $L_{C0} = 300 \text{ nm}$  ( $t_{SC} = 50 \text{ nm}$ ),  $L_{C0} = 600 \text{ nm}$  ( $t_{SC} = 100 \text{ nm}$ ),  $L_{C0} = 900 \text{ nm}$  ( $t_{SC} = 150 \text{ nm}$ ) and  $L_{C0} = 1200 \text{ nm}$  ( $t_{SC} = 200 \text{ nm}$ ). This relationship is expected to hold for thicker films, but thin semiconductor films are often of greater interest.

Large contacts are then required to afford greater charge injection (diffusion) in order to fulfil the channel transport. Compared to  $R_{sd}$ , this OSC film thickness effect is smaller for  $R_{ch}$  and thus a contact length of  $L_{C0} = 6t_{SC}$  is enough for the lowest contact resistance and negligible influence on the channel transport.

As  $L$  is scaled down, the channel becomes more current demanding, but the current supplied by contacts is not amplified if  $L_C$  remains constant. In this case, the whole contact surface will be involved in charge injection, i.e.,  $L_{C0} = L_C$ , and the apparent transistor characteristics become contact limited. This effect will be significant under high gate biases as the channel is highly conductive. Enlarging contacts ( $L_C$ ) and thus the effective charge injection area ( $L_{C0}$ ) ameliorates such a contact limitation, providing more current to the “current hungry” channel. A contact length  $L_C = 0.6\mu\text{m}$  is able to ensure the lowest  $R_{sd}$ . Yet, the short channels necessitate large contacts, potentially exceeding the presumption of  $L_{C0} = 6t_{sc}$ . An interesting implication of this result is that in future nano-scale transistors,  $L_{C0}$  will become the primary consideration for proper channel transport rather than for the lowest contact resistance.

A large-size contact compensates for the decreased efficiency of charge injection at the interface and the charge migration in the OSC bulk, reducing the contact resistance and the relevant contact effects as well. Contact limitation that manifests as an elevated  $R_{ch}$  arises only with small  $L_C$ . Finally, we can conclude that if the transport is mostly by hopping or the carrier mobility is highly anisotropic.

Drain current increases with increasing the contact length but in contact length  $10\mu\text{m}$  and less drain current value is very low. Therefore contact length is greater than  $10\mu\text{m}$ . Best suitable contact length for this top contact geometry is  $30\mu\text{m}$ .

In bottom contact the variation in channel length  $10\mu\text{m}$  and  $20\mu\text{m}$  shows abnormal characteristic because in bottom contact the charge injection area is near the contact current crowding is more if channel length is small. Best suitable channel length for bottom contact is  $30\mu\text{m}$ .

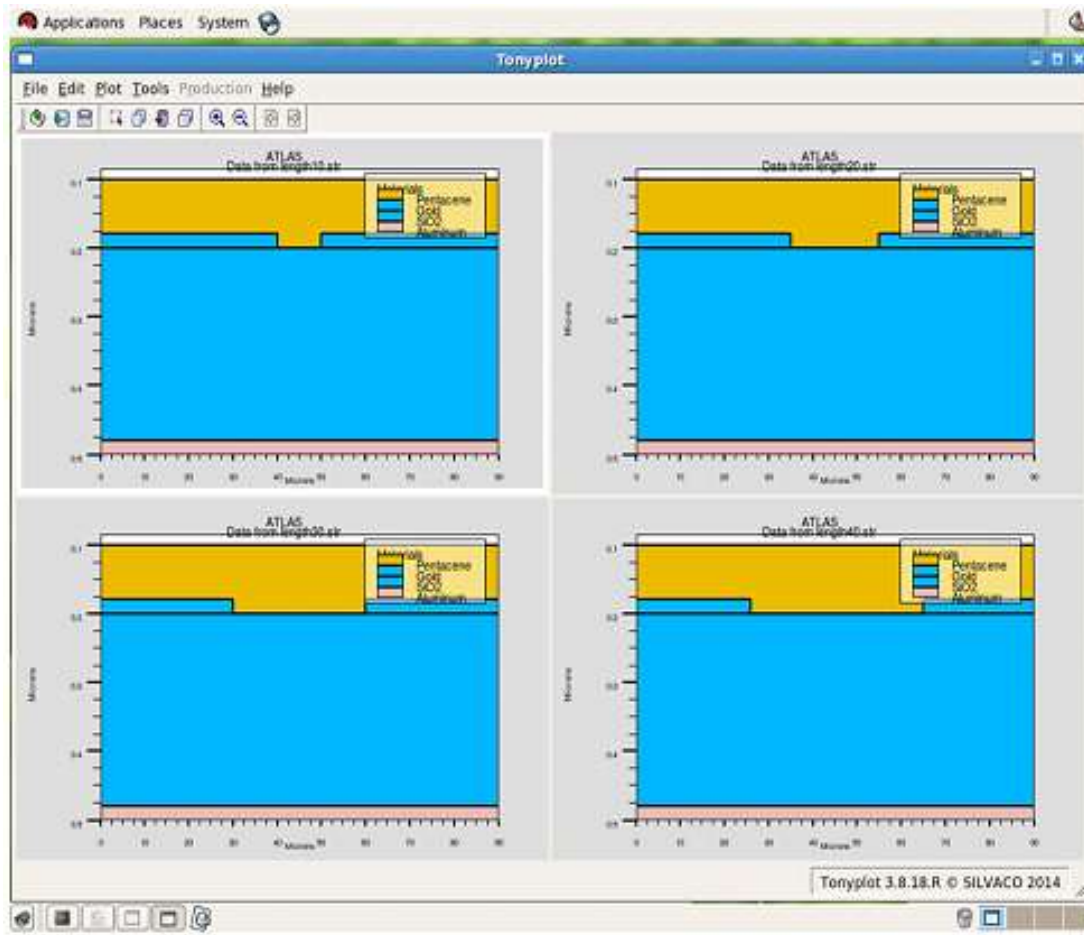


**Figure 5-0-1 Tonyplot Of Bottom Contact Ofet With 10, 20, 30 & 40 Micrometer Channel Lengths**

This study represents the variation in channel length in bottom contact geometry with 10, 20, 30 & 40 micro meter contact lengths. As shown in the figure . Higher contact length reduces contact resistance but large contacts greatly increase the device size and consume more contact material. Parameters used in the structure of the OFET are length of the device is 90  $\mu\text{m}$ . Width of the gate is 20 nm and material used is aluminium, width of the gate oxide is 280 nm material used is  $\text{SiO}_2$ , organic material is pentacene thickness of pentacene is 280 nm, source and drain thickness is 20 nm or less length is varied over 10  $\mu\text{m}$  to 40  $\mu\text{m}$ .



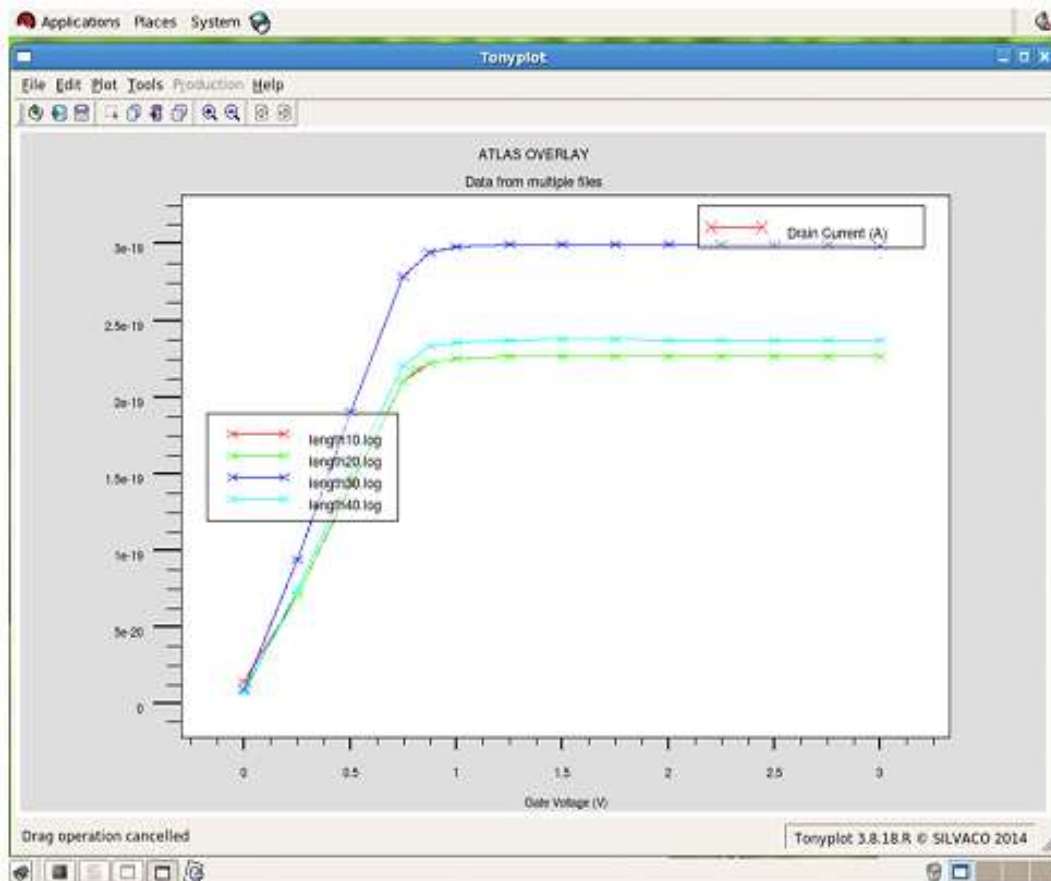


**Figure 5-0-2 Tonyplot Of Id-Vg characteristics Of Bottom Contact Ofet With 10, 20, 30 & 40 micrometer Channel Lengths**

This study represents the variation in contact length in bottom contact geometry with 10, 20, 30 & 40 micrometer contact lengths. As shown in the figure increasing the contact length drain current increases. In 10 micrometer contact length drain current value is very small so not suitable for the geometry and in 40 micrometer contact length the value of drain current is less than the 30 micrometer contact length. In this case the best suitable contact length is 30 micrometer.

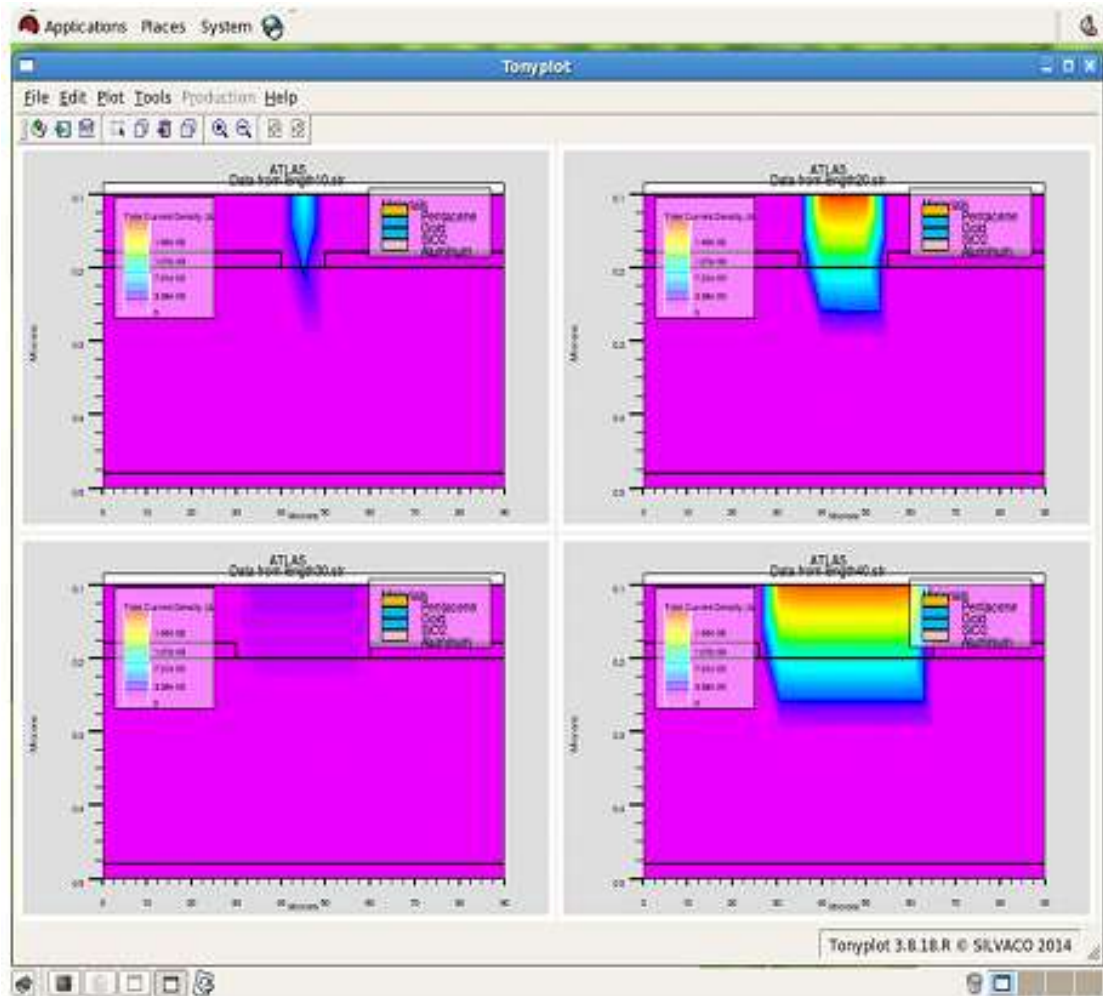


Figure 5-0-3Tony plot of Total Current Density in bottom contact lengths of ofet.

It is defined as a vector whose magnitude is the electric **current** per cross-sectional area at a given point in space (i.e. it is a vector field). In SI units, the electric **current density** is measured in amperes per square metre.

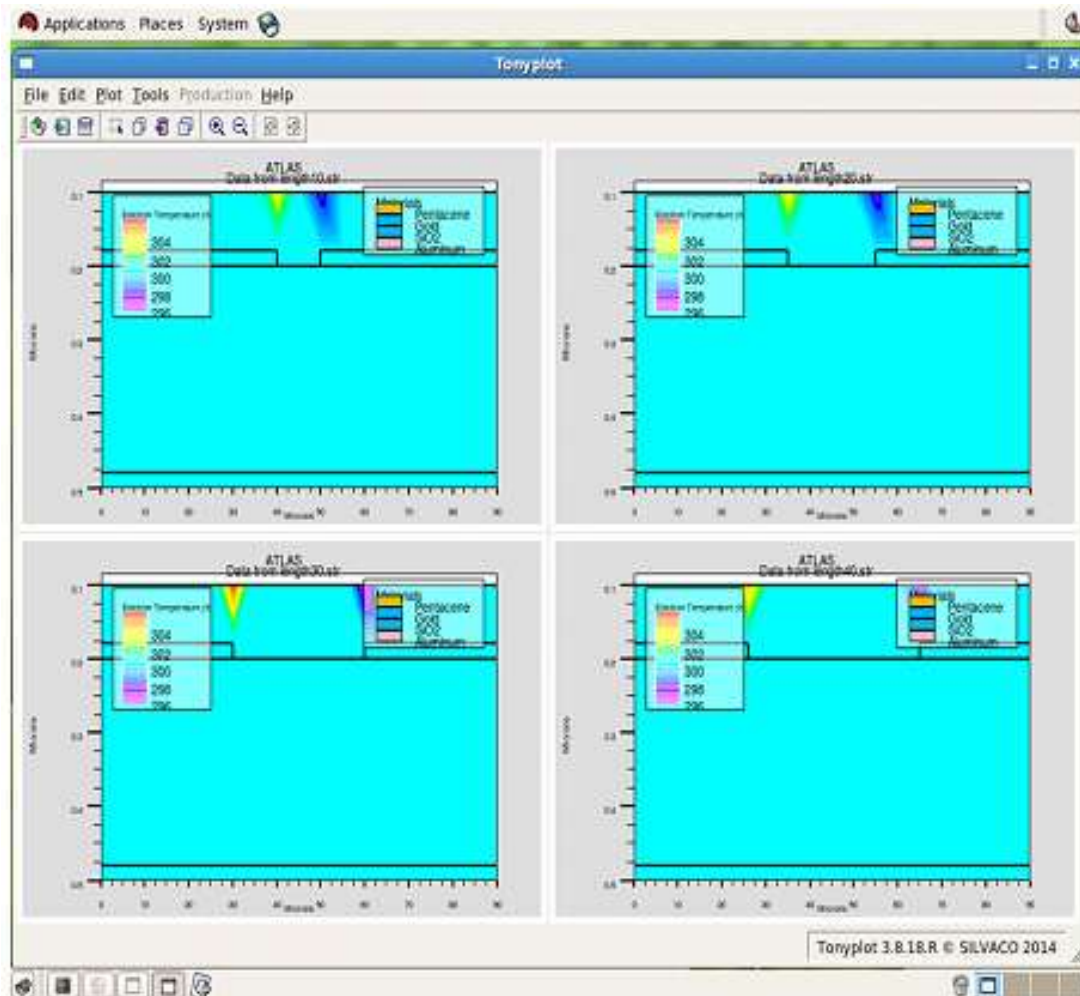
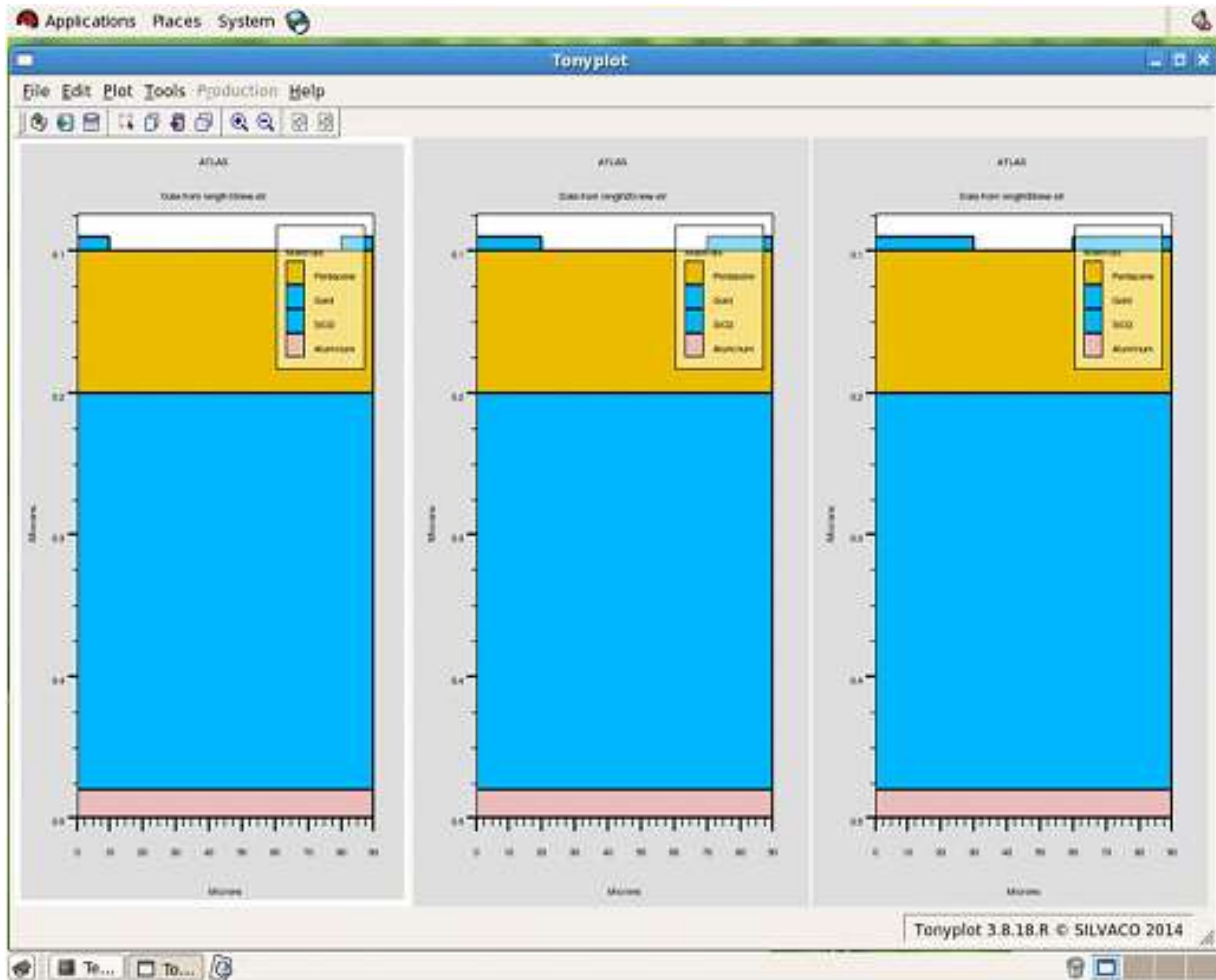


Figure 5-0-4 Tony plot of Electron Temperature in bottom contact lengths of ofet.

The average specifically means to average over the kinetic energy of all the particles in your system. If the velocities of a group of electrons, e.g., in a plasma, follow a Maxwell Boltzmann distribution, then the **electron temperature** is well-defined as the **temperature** of that distribution.



**Figure 5-0-5 Tony plot Of Top Contact Ofet With 10,20 & 30 Micrometer Contact Lengths**

This study represents the variation in channel length in bottom contact geometry with 10, 20 & 30 micrometer contact lengths. As shown in the figure higher contact length reduces contact resistance but large contacts greatly increase the device size and consume more contact material. Parameters used in the structure of the OFET are length of the device is 90  $\mu\text{m}$ . Width of the gate is 20 nm and material used is aluminium, width of the gate oxide is 280 nm material used is  $\text{SiO}_2$ , organic material is pentacene thickness of pentacene is 280 nm, source and drain thickness is 20 nm or less length is varied over 10  $\mu\text{m}$  to 30  $\mu\text{m}$ . Here we have not taken 40  $\mu\text{m}$  contact length because it consumes more gold.

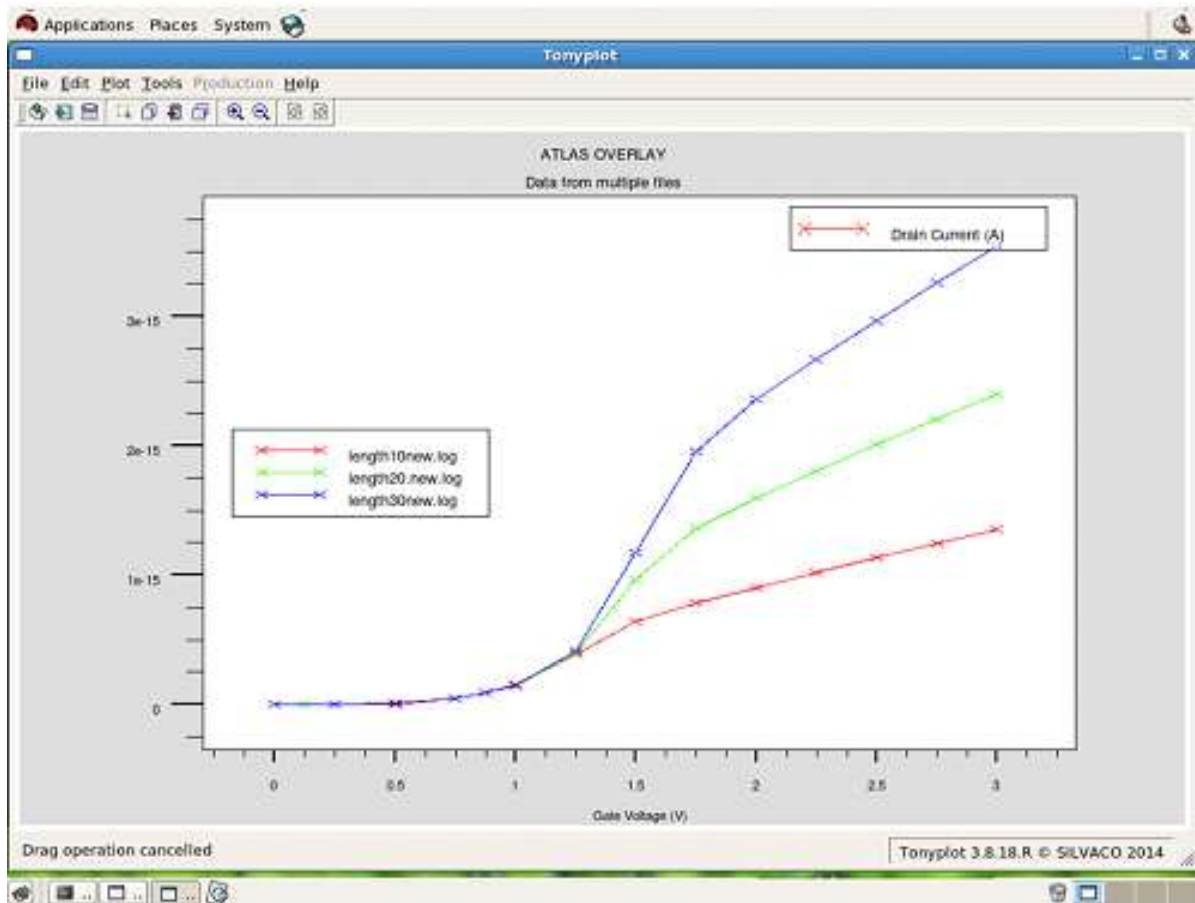


Figure 5-0-6 Tonyplot Of Id-Vg characteristics Of Top Contact Ofet With 10,20 & 30 Micrometer Contact Lengths

This study represents the variation in contact length in top contact geometry with 10, 20 & 30 micro meter contact lengths. As shown in the figure increasing the contact length drain current increases. In 10 micrometer contact length drain current value is very small so not suitable for the geometry and in 40 micrometer contact length the quantity of gold used in source and drain increases so not suitable for the geometry. In this case the best suitable contact length is 30 micrometer.

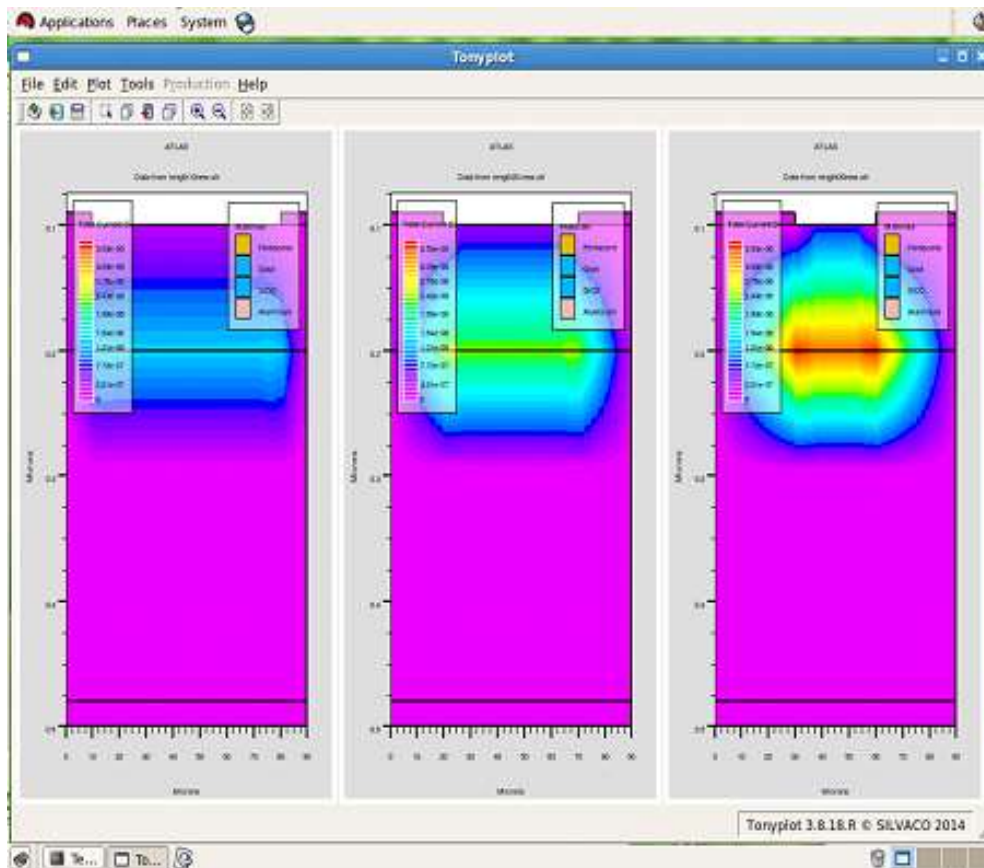


Figure 5-7 Tony plot of Total Current Density in top contact lengths of ofet.

It is defined as a vector whose magnitude is the electric **current** per cross-sectional area at a given point in space (i.e. it is a vector field). In SI units, the electric **current density** is measured in amperes per square metre

## **CHAPTER 6 CONCLUSION AND FUTURE WORK**

### **CONCLUSION**

In summary this study represents the variation in contact length in top contact geometry and channel length variation in bottom contact geometry. As shown in the figure that increasing the contact length the value of drain current is increased. Best suitable for top contact is  $30\mu\text{m}$  or contact length is greater than or equal to  $10\mu\text{m}$ . In bottom contact channel length modulation is carried out. The contact length must be greater than  $10\mu\text{m}$  i.e. channel length must be smaller than  $70\mu\text{m}$  for other values graph shows abnormal behaviour. In this case also the best suitable contact length is  $30\mu\text{m}$ .

### **FUTURE WORK**

To make pentacene as n-type by adding gate insulator polyvinyl alcohol (PVA). It gives electron to the accumulation layer. Thus pentacene behaves as n-type also. With this n-type and p-type from same material it is easy for complementary structures fabrication. Logic gates can be designed with this. There are a series of approaches to make organic Field effect transistor ambipolar: 1. Single -component transistors, by employing a material which is able to transport both charges, 2. bilayer, by depositing two organic materials one on top of the other and 3. blend, by mixing together the two components.

To examine the device characteristics as a function of organic semiconductor thickness based on this the values for Electrical potential profile, Carrier density and I-V characteristics.

To use pentacene with different dielectrics (Cyanoethylpullulane, Poly(4-vinylphenol), Polymethyl methacrylate, Polyimide & Parylene-C) as gate insulators & then to examine the Sub threshold slope, On-state drain current, Threshold voltage and Carrier mobility.

## REFERENCES

- [1]. F. Gutmann and L. E. Lyons, *Organic Semiconductors*. John Wiley & Sons, Inc, 1967.
- [2]. W. F. Pasveer, *Charge and Energy Transport in Disordered  $\pi$ -conjugated Systems*. PhD thesis, Technische Universiteit Eindhoven, 2004.
- [3]. F. Garnier, "Scope and limits of organic-based thin-film transistors," *Phil. Trans.*, vol. 355, pp. 815-827, 1997.
- [4]. J. M. Shaw and P. F. Seidler, "Organic electronics: Introduction," *IBM J. Res. Dev.*, vol. 45, pp. 3-9, 2001.
- [5]. "Organic semiconductor world," <http://www.iapp.de/orgworld>.
- [6]. A. Pochettino, "Sul comportamento foto-elettrico dell' antracene," *Acad. Lincei Rendic.* 15, 355, 1906.
- [7]. J. Koenigsberger and K. Schilling, "Über Elektrizitätsleitung in festen Elementen und Verbindungen", *Annalen der Physik* 32, 179, 1910.
- [8]. C. K. Chiang, C. R. Fincher, Y. W. Park, A. J. Heeger, H. Shirakawa, E. J. Louis, S. C. Gau, and A. G. MacDiarmid, "Electrical conductivity in doped polyacetylene," *Physical Review Letters* 39, 1098, 1977.
- [9]. "Introducing World's First OLED TV," [www.sonymstyle.com/oled](http://www.sonymstyle.com/oled).
- [10]. B. C. Thompson and J. M. J. Fréchet, "Polymer-fullerene composite solar cells," *Angewandte Chemie International Edition* 47, 58-77, 2008.
- [11]. V. Subramanian, J. M. J. Frechet, P. C. Chang, D. C. Huang, J. B. Lee, S. E. Molesa, A. R. Murphy, D. R. Redinger, and S. K. Volkman, "Progress toward development of all-printed RFID tags. Materials, processes, and devices," *Proceedings of the IEEE* 93, 1330-1338, 2005.
- [12]. G. H. Gelinck, H. E. A. Huitema, E. van Veenendaal, E. Cantatore, L. Schrijnemakers, J. B. P. H. van der Putten, T. C. T. Geuns, M. Beenhakkers, J. B. Giesbers, B.-H. Huisman, E. J. Meijer, E. M. Benito, F. J. Touwslager, A. W. Marsman, B. J. E. van Rens, and D. M. de Leeuw, "Flexible active-matrix displays and shift registers based on solution-processed organic transistors," *Nature Materials* 3, 106-110, 2004.
- [13]. L. Zhou, A. Wang, S.-C. Wu, J. Sun, S. Park, and T. N. Jackson, "All-organic active matrix flexible display," *Applied Physics Letters* 88, 083502/1-083502/3, 2006.
- [14]. T. W. Kelley, L. D. Boardman, T. D. Dunbar, D. V. Muyres, M. J. Pellerite, and T. P. Smith, "High-performance OTFTs using surface-modified alumina dielectrics," *Journal of Physical Chemistry B* 107, 5877-5881, 2003.



- [15]. C. R. Kagan and P. Andry, *Thin-Film Transistors*, 1st ed. Boca Raton, FL, USA: CRC Press, 2003.
- [16]. Yoshiro Yamashita, “Organic semiconductors for organic field-effect transistors”, a review of *Sci. Technol. Adv. Mater.* 10 (2009) 024313 (9pp).
- [17]. E. J. Meijer, D. M. D. Leeuw, S. Setayesh, E. van Veenendaal, B.-H. Huisman, P.W. M. Blom, J. C. Hummelen, U. Scherf, and T. M. Klapwijk, “Solution-processed ambipolar organic field-effect transistors and inverters,” *Nat. Mater.*, vol. 2, pp. 678- 682, 2003.
- [18]. T. Anthopoulos, C. Tanase, S. Setayesh, E. J. Meijer, J. C. Hummelen, P. W. M. Blom, and D. M. D. Leeuw, “Ambipolar organic field-effect transistors based on solution processed methanofullerene,” *Adv. Mater.*, vol. 16, pp. 2174-2179, 2004.
- [19]. Simone Locci, *Modeling of the Physical and Electrical Characteristics of Organic Thin Film Transistors* PhD thesis, 2009.
- [20]. J. C. Scott, “Metal-organic interface and charge injection in organic electronic devices,” *J. Vac. Sci. Technol. A.*, vol. 21, pp. 521-531, 2003.
- [21]. Gilles Horowitz, *Organic Field-Effect Transistors*, *Advance Material* 1998.
- [22]. K.P. Pernstich, S. Haas, D. Oberhoff, C. Goldmann, D.J. Gundlach, B. Batlogg, A.N. Rashid, and G. Schitter, “Threshold voltage shift in organic field effect transistors by dipole monolayers on the gate insulator”, *J. Appl. Phys.* 96, 6431-6438 (2004).
- [23]. A. Knobloch, A. Manuelli, A. Bernds, and W. Clemens, “Fully printed integrated circuits from solution processable polymers”, *J. Appl. Phys.* 96, 2286-2291 (2004).
- [24]. D. Kim, S. Jeong, J. Moon, S. Han, and J. Chung, “Organic thin film transistors with ink-jet printed metal nanoparticle electrodes of a reduced channel length by laser ablation”, *Appl. Phys. Lett.* 91, 071114 (2007).
- [25]. T.D. Anthopoulos, D.M. de Leeuw, E. Cantatore, P. van't Hof, J. Alma, and J.C. Hummelen, “Solution processible organic transistors and circuits based on a C70 methanofullerene”, *J. Appl. Phys.* 98, 054503 (2005).
- [26]. N.J. Pinto, R. Perez, C.H. Mueller, N. Theofylaktos, and F.A. Miranda, “Dual input AND gate fabricated from a single channel poly 3-hexylthiophene thin film field effect transistor”, *J. Appl. Phys.* 99, 084504 (2006).
- [27]. G. Gu, M.G. Kane, and S.C. Mau, “Reversible memory effects and acceptor states in pentacene-based organic thinfilm transistors”, *J. Appl. Phys.* 101, 014504 (2007).
- [28]. S.H. Hur, C. Kocabas, A. Gaur, O. Ok Park, M. Shima, and J.A. Rogers, “Printed

thin-film transistors and complementary logic gates that use polymer-coated single-walled carbon nanotube networks”, *J. Appl. Phys.* 98, 114302 (2005).

[29]. T.B. Singh, P. Senkarabacak, N.S. Sariciftci, A. Tanda, C. Lackner, R. Hagelauer, and G. Horowitz, “Organic inverter circuits employing ambipolar pentacene field effect transistors”, *Appl. Phys. Lett.* 89, 033512–4 (2006).

[30]. K. Hummelen. Reader preparation of nanomaterials and devices, topmaster nanoscience, part1 Synthesis of functional molecules (RuG, 2004).

[31]. C. Mattheus. Polymorphism and electronic properties of pentacene. Ph.D. thesis, RUG (2002).

[32]. O. D. Jurchescu, J. Baas, and T. Palstra. Effects of impurities of single crystal pentacene. *Appl. Phys. Lett* 84, 3061 (2004).

[33]. A. Schoonveld. Transistors based on ordered organic semiconductors. Ph.D. thesis, RUG (1999).

[34]. O. D. Jurchescu, J. Baas, and T. Palstra. Electronic transport properties of pentacene single crystals upon exposure to air. to be published 0, 0 (2005).

[35]. J. E. Northrup and L. Chabiny. Gap states in organic semiconductors: Hydrogen- and oxygen-induced states in pentacene. *Phys. Rev. B.* 68, 0412021 (2003).

[36]. D. Li, E. Borkent, R. Nortrup, H. Moon, H. Katz, and Z. Bao. Humidity effect on electrical performance of organic thin-film transistors. *Appl. Phys. Lett* 86, 0421051 (2005).

[37]. A. Vollmer, O. D. Jurchescu, I. Arfaoui, T. Palstra, P. Rudolf, J. Niemax, J. Pflaum, I. Salzman, J. P. Rabe, and N. Koch. The effect of oxygen exposure on pentacene electronic structure. to be published 0, 0 (2005).

[38]. T. Minari, T. Nemoto, and S. Isoda. Fabrication and characterization of single-grain organic field-effect transistor. *J. Appl. Phys.* 96, 769 (2004).

[39]. C. Tanase. Unified Charge Transport in Disordered Organic Field-Effect Transistors and Light- Emitting diodes. Ph.D. thesis, RUG (2005)

[40]. P. V. Pesavento, R. J. Chesterfield, C. R. Newman, and C. D. Frisbie. Gated four-probe measurements on pentacene thin-film transistors: Contact resistance as a function of gate voltage and temperature. *J. Appl. Phys.* 96, 7312 (2005).

[41]. M. Popinciuc, H. T. Jonkman, and B. J. van Wees. . to be published (2005).

[42]. C. Rost, S. Karg, W. Riess, M. A. Loi, M. Murgia, and M. Muccini. Light-emitting ambipolar organic heterostructure field-effect transistor. *Synthetic Metals* 146, 237 (2004).

[43]. T. Yasuda, T. Goto, K. Fujita, and T. Tsutsui. Ambipolar pentacene field-effect transistors with calcium source drain electrodes. *Appl. Phys. Lett* 85, 2098 (2004).

[44]. M.J. MAŁACHOWSKI<sup>1</sup> and J. ŻMIJA Organic field-effect transistors *OPTO-ELECTRONICS REVIEW* 18(2), 121-136.

[45]. ATLAS user manual.

[46]. *Physical and Chemical Aspects of Organic Electronics* edited by Christof Wöll page 306-307.

[47]. *Physics of Organic Semiconductors* edited by Wolfgang Brütting, Chihaya Adachi page no 34- 36.

[48]. Yong Xu Chuan Liu , William Scheideler , Peter Darmawan , Songlin Li , Francis Balestra , Gerard Ghibaudo , Kazuhito Tsukagoshi *Organic Electronics* 14 (2013) 1797-1804.

